

# Quantum optical lattices for emergent many-body phases of ultracold atoms

Santiago F. Caballero-Benitez and Igor B. Mekhov

*University of Oxford, Department of Physics, Clarendon Laboratory, Parks Road, Oxford OX1 3PU, UK*

Ultracold atoms in optical lattices allow looking in the quantum realm with an undeniable control, which enabled numerous interdisciplinary discoveries. However, studies of systems trapped in prescribed potentials created by classical laser beams start meeting their boundaries. Here we make a step further, introducing the quantumness of light. We show that novel emergent phases appear not only due to the coupled light-matter dynamics, but even solely due to quantum correlations between them. We suggest mechanisms for imprinting quantum patterns on many-body nonlocal interactions of atoms. Even using single-mode cavities, the patterns are spatially multimode. This induces various types of orders because symmetries are broken and inherited from light. We show that competition between light-field and matter-field coherences leads to novel phases (e.g. delocalized dimers), beyond density-induced orders such as multimode generalizations of density waves and supersolid-like states. Some phases can be protected by an energy gap, thus having topological character.

Ultracold atoms trapped in optical lattices enable to study quantum many-body phases with undeniable precision and target problems from several disciplines [1]. Such optical potentials can be complicated, but are prescribed, i.e., they are created by external lasers and are not sensitive to atomic phases. This limits the range of obtainable phases. The self-consistent light-matter states can be obtained, when scattered light modifies the trapping potential itself. This was achieved by trapping a Bose-Einstein condensate (BEC) inside an optical cavity [2–4], which dramatically enhances the light-matter coupling, thus making the influence of reemission light comparable to that of external lasers. Such "dynamical potentials" [5] enabled the structural Dicke phase transition and a state with supersolid properties [2]. A key effect observed so far, is the dynamical dependence of light intensity (potential depth) on the atomic density. Although, the light becomes dynamical, its quantum properties are still not totally exploited as works on atomic motion in quantum light were limited to few atoms [6–9]. Effects in dynamical potentials are analogous to semiclassical optics, where atomic excitations are quantum, while light is still classical. As the light and BEC are quantum objects, the quantum fluctuations of both were studied [10, 11], however, the fundamental reason of the structural phase transition can be traced back to the dynamical self-organization predicted [12] and observed [13] with thermal atoms and classical light. For single-mode cavities, dynamical light-matter coupling was shown to lead to several effects [14–18] yet to be observed. Multimode cavities extend the range of quantum phases further [8, 19, 20].

Here we show that, even in a single-mode cavity, the quantum potential [6, 21, 22] leads to significant many-body effects beyond semiclassical ones. Multimode spatial patterns of matter fields arise due to symmetry breaking resulting from the competition between imposed global light structure and standard local processes (tunneling and on-site interactions). We prove that many-body states are not limited to the density-induced orders as in previous studies, but also represent long-range pat-

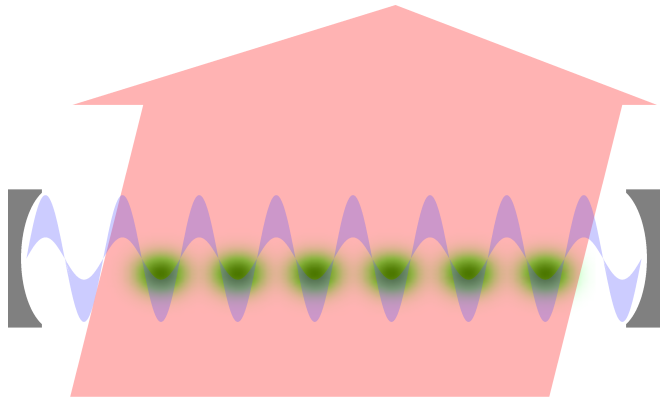


FIG. 1: **Cold atoms trapped in an optical lattice subject to a quantum potential created by the light inside a single-mode cavity.** The unsharp potential contour schematically depicts quantum fluctuations of light, which induce the light-matter correlations. The cavity can be a standing- or travelling-wave one.

terns of matter-field coherences (bonds [23]), leading, for example, to far delocalized dimers. Recently, nontrivial spatial patterns were obtained with classical atoms and light [24]. Our work will assist to extend such effort in the interdisciplinary field of optomechanics towards quantum multimode systems [25]. The mechanisms we suggest, provide a general framework and a new set of tools, inaccessible in setups using classical optical lattices. Therefore, this merges quantum optics and quantum many-body systems at the fully quantum level of light-matter interaction. This will strongly expand applications in quantum simulators and quantum information. It will allow exploring fundamental issues concerning emergence of multimode generalizations of strongly correlated phases, such as gapped superfluids [26] and density waves [27] as well as their interplay, giving rise to quantum solids [28]. We find the essential ingredients to control these phases. The light-induced structure is similar to multi-component nonlinear sigma mod-

els ubiquitous in analog models of high-energy [29, 30], condensed matter [31, 32], and relativistic [33] physics. Dimer phases can be used as building blocks for quantum spin-liquids simulations [34].

We consider atoms trapped in an optical lattice inside single-mode cavity with the mode frequency  $\omega_c$  and decay rate  $\kappa$  in off-resonant scattering (see Fig. 1). The pump light with the amplitude  $a_0$  and frequency  $\omega_p$  ( $\Delta_p = \omega_p - \omega_c$ ) illuminates atoms in a plane transverse to the cavity axis, but not necessarily at  $90^\circ$ . The atoms couple with light via the coupling strength  $g_2 = a_0 g^2 / \Delta_a$ , where  $g$  is the light-matter coupling coefficient and  $\Delta_a$  is the detuning between the light and atomic resonance [22, 35, 36]. This can be described by the Hamiltonian  $\mathcal{H} = \mathcal{H}^b + \mathcal{H}^a + \mathcal{H}^{ab}$ , where  $\mathcal{H}^b$  is the regular Bose-Hubbard (BH) Hamiltonian (see Methods). The light is described by  $\mathcal{H}^a = \hbar \omega_c \hat{a}^\dagger \hat{a}$  and the light-atom interaction is [22]:

$$\mathcal{H}^{ab} = g_2 \hat{a} \hat{F}^\dagger + g_2^* \hat{a}^\dagger \hat{F} \quad (1)$$

with  $\hat{F} = \hat{D} + \hat{B}$ .  $\hat{D} = \sum_j J_{j,j} \hat{n}_j$  is the diagonal coupling of light to on-site densities,  $\hat{B} = \sum_{\langle i,j \rangle} J_{i,j} (\hat{b}_i^\dagger \hat{b}_j + h.c.)$  is the off-diagonal coupling to the inter-site densities reflecting matter-field interference, or "bonds" [35]. The sums go over the illuminated sites  $N_s$ ,  $\langle i,j \rangle$  refers to nearest neighbour pairs. The operators  $\hat{a}^\dagger$  ( $\hat{a}$ ) create (annihilate) photons in the cavity while  $\hat{b}_i^\dagger$  ( $\hat{b}_i$ ) correspond to bosonic atoms at site  $i$  of the optical lattice (OL).  $\mathcal{H}^{ab}$  is a consequence of the quantum potential seen by atoms on top of the BH model given by a classical OL with the hopping amplitude  $t_0$  and on-site interaction  $U$ .

The spatial structure of light gives a natural basis to define the atomic modes, as the coupling coefficients  $J_{i,j}$  (see Methods) can periodically repeat in space. The symmetries broken in the system are inherited from such a periodicity: all atoms equally coupled to light belong to the same mode, while the ones coupled differently belong to different modes. We define operators corresponding to modes  $\varphi$ :  $\hat{F} = \sum_\varphi \hat{D}_\varphi + \sum_{\varphi'} \hat{B}_{\varphi'}$ , where

$$\hat{D}_\varphi = J_{D,\varphi} \hat{N}_\varphi, \text{ with } \hat{N}_\varphi = \sum_{i \in \varphi} \hat{n}_i, \quad (2)$$

$$\hat{B}_{\varphi'} = J_{B,\varphi'} \hat{S}_{\varphi'}, \text{ with } \hat{S}_{\varphi'} = \sum_{\langle i,j \rangle \in \varphi'} (\hat{b}_i^\dagger \hat{b}_j + h.c.). \quad (3)$$

Thus, we replaced the representation of atomic operator  $\hat{F}$  as a sum of microscopic on-site and inter-site contributions by the smaller sum of macroscopically occupied global modes with number density,  $\hat{N}_\varphi$ , and bond,  $\hat{S}_{\varphi}$ , operators. The structures of density and bond modes can be nearly independent from each other. To be precise, for the homogeneous scattering in a diffraction maximum,  $J_{i,j} = J_B$  and  $J_{j,i} = J_D$ , one spatial mode is formed. When light is scattered in the main diffraction minimum (at  $90^\circ$  to the cavity axis), the pattern of light-induced modes alternates sign as in the staggered field,  $J_{i,j} = J_{j,i} = (-1)^j J_B$  and  $J_{j,j} = (-1)^j J_D$ . This gives

two spatial density modes (odd and even sites) and, as we will show, four bond modes. It is possible to decouple the density and bond modes by choosing angles such that  $J_D = 0$  or  $J_B = 0$  [35]. Beyond this, additional modes get imprinted by pumping light at different angles such that each  $R$ -th site or bond scatter light with equal phases and amplitudes. This generates multimode structures of  $R$  density modes [36, 37] and  $2R$  bond modes. The prominent example of self-organization [12, 15–17] is thus a special case of two density modes, while macroscopic effects related to the higher density modes and any bond modes have not been addressed so far.

In general, the light and matter are entangled [6, 21, 38–40]. In the steady state of light, it can be adiabatically eliminated and the full light-matter state can be then reconstructed as we will show later. The effective atomic Hamiltonian [6, 15, 22] is

$$\mathcal{H}_{\text{eff}}^b = \mathcal{H}^b + \frac{g_{\text{eff}}}{2} (\hat{F}^\dagger \hat{F} + \hat{F} \hat{F}^\dagger), \quad (4)$$

where  $g_{\text{eff}} = \Delta_p |g_2|^2 / (\Delta_p^2 + \kappa^2)$ . A key physical processes is that the ground state is reached (i.e. the energy in Eq. (4) is minimized), when the system adapts (self-organize) in such a way that the light scattering term is maximized for  $\Delta_p < 0$ , and minimized for  $\Delta_p > 0$ . New terms beyond BH Hamiltonian give the effective long-range light-induced interaction between density and bond modes:

$$\begin{aligned} \hat{F}^\dagger \hat{F} + \hat{F} \hat{F}^\dagger &= \sum_{\varphi, \varphi'} (J_{D,\varphi}^* J_{D,\varphi'} + c.c.) \hat{N}_\varphi \hat{N}_{\varphi'} \\ &+ (J_{B,\varphi}^* J_{B,\varphi'} + c.c.) \hat{S}_\varphi \hat{S}_{\varphi'} \\ &+ (J_{D,\varphi}^* J_{B,\varphi'} + c.c.) \hat{N}_\varphi \hat{S}_{\varphi'} \\ &+ (J_{B,\varphi}^* J_{D,\varphi'} + c.c.) \hat{N}_\varphi \hat{S}_{\varphi'}. \end{aligned} \quad (5)$$

Thus, any symmetry broken by the light modes imprints the structure on the interaction of atomic modes. The "on-mode" terms  $\sum_\varphi (\hat{F}_\varphi^\dagger \hat{F}_\varphi + h.c.)$  resemble a structure in the nonlinear sigma model with modified constraints [31]. In general, effective field theories can have non-Abelian components and are nonlocal.

We decompose the light-induced interaction (5) in mean-field contributions and fluctuations:

$$\hat{F}^\dagger \hat{F} + \hat{F} \hat{F}^\dagger = \langle \hat{F}^\dagger \hat{F} \rangle + \langle \hat{F} \hat{F}^\dagger \rangle + \delta \hat{F}^\dagger \hat{F}, \quad (6)$$

where  $\langle \cdot \rangle$  is the expectation value. The last term  $\delta \hat{F}^\dagger \hat{F}$  originates from the quantum light-matter correlations, underlying the quantumness of OL. Other terms originate from the dynamical but classical light, when the semiclassical approximation  $\hat{a} \hat{F}^\dagger = \langle \hat{a} \rangle \hat{F}^\dagger$  holds. Decoherating operators at different sites, we obtain a mean-field theory that has nonlocal coupling between the matter modes and is local in fluctuations (see Methods). In particular, for  $\delta \hat{D}^\dagger \hat{D}$  these reduce to on-site atom number fluctuations. Importantly, this corresponds to the

purely light-induced effective on-site interaction of atoms beyond the standard BH term. For  $\delta\hat{B}^\dagger\hat{B}$ , light-matter correlations reduce to two- and three-point tunneling correlations, while four-point correlations contribute to the semiclassical term. These are the sum over terms like  $\hat{b}_i^\dagger\hat{b}_j\hat{b}_k^\dagger\hat{b}_l$ , which include radically new terms beyond BH model: fluctuations of the order parameter and density-density coupling between neighbouring sites. Strikingly, the effective mean-field Hamiltonian leads not only to the renormalization of the BH constants, but also to the appearance of new terms that couple densities, order parameters and their fluctuations. In contrast to previous works, we will show non-negligible effects due to such terms.

When the ground state of  $\mathcal{H}_{\text{eff}}^b$  is achieved by maximizing scattering ( $\Delta_p < 0$ ), a strong classical light emerges and small fluctuations can be neglected. The quantum matter fields self-organize to maximize the scattering, and we will demonstrate novel multimode density patterns. Moreover, the bond self-organization physically corresponds to a nontrivial structure in the phases of complex matter-fields  $\hat{b}_i$  (with complex order parameters  $\psi_i = \langle \hat{b}_i \rangle$ ), beyond simpler density patterns. It can be observed in the nontrivial structure of matter-field interferences between the sites [35]. In principle, even in the strong-light case, the light quantumness can play a role, because the self-organized states can be in a superposition of several patterns and different light amplitudes are correlated to them [6]. Nevertheless, in a realistic case with dissipation, the system quickly collapses to one of the semiclassical states [41]. We will show that quantum fluctuations play a key role in an opposite case, where scattering is minimized ( $\Delta_p > 0$ ) such that no classical light builds at all, but light fluctuations design the emergence of novel phases. Quantum nature of atoms gives massively degenerate states which depend on how many symmetries are broken. As symmetries are broken and fluctuations affected, the degeneracy gets suppressed. These features determine formation of macroscopic orders either topological or conventional. To underline fundamental phenomena, we will consider cases with only either density or bond modes. Their interplay is indeed interesting, but less intuitive and will be reported elsewhere.

We start with the simplest case of homogeneous scattering with no symmetry broken (in a diffraction maximum all  $J_D$ 's are equal,  $J_B = 0$ ). Density-dependent classical light was previously shown to strongly modify the standard phase diagram of Mott insulator (MI) - superfluid (SF) transition [14, 15], if plotted via the chemical potential  $\mu$ . Here we chose to present phase diagrams via the density  $\rho$ , which hides most of such classical effects, but in turn underlines novel phenomena, we are focused on. At fixed density per site, the quantum light-matter correlations effectively renormalize the on-site interaction from  $U$  to  $U + 2g_{\text{eff}}J_D^2$  (see Fig. 2a and Methods). Thus, changing the light-matter coupling, one can shift the SF-MI transition point. This is be-

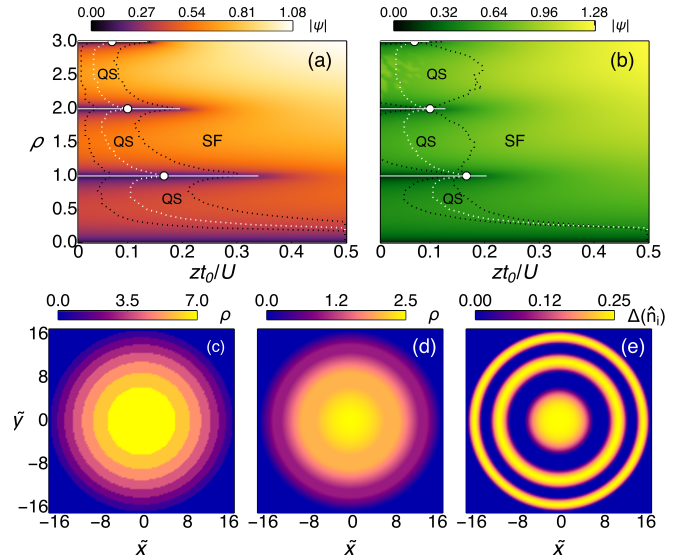


FIG. 2: **Modifications of quantum phases due to quantum and semiclassical effects for homogenous scattering.** (a) Phase diagram in terms of SF order parameter  $\psi$  at fixed density for density-induced scattering. For minimal (maximal) scattering, MI boundaries (white lines) become extended (shortened) with respect to the transition point without cavity light (white point). This corresponds to suppression (enhancement) of quantum-light-induced atomic fluctuations. The behaviour of boundaries of the gapped QS state is similar (black dotted lines). The white dotted line is for gapless QS without cavity light. (b) Phase diagram for off-diagonal bond-induced scattering. The processes and lines are similar to (a), but arise due to renormalization of the tunnelling amplitude resulting from semiclassical light scattering. (c) Density profile  $\rho$  in a very deep OL without cavity light. Harmonic confinement in 2D leads to MI states with standard "wedding cake" structure. On-site fluctuations are zero everywhere. (d) Density profile  $\rho$  and (e) on-site atom number fluctuations  $\Delta(\hat{n}_i) = \langle (\hat{n}_i - \rho)^2 \rangle$  in the system with quantum light for a very deep OL. Regions with fluctuations ( $\Delta(\hat{n}_i) \neq 0$ ) and smooth density variations correspond to gapped QS states, which do not exist in standard BH model in (c). The trapping potential is  $V_T(r) = 0.025U(\tilde{x}^2 + \tilde{y}^2)$ ,  $\tilde{x} = x/a$ ,  $\tilde{y} = y/a$  with  $a$  is the lattice spacing;  $\mu = 7U$ . Parameters: (a)  $g_{\text{eff}} = 25U/N_s$ , the boundaries are for  $g_{\text{eff}} = 25U/N_s$ , 0, and  $-12.5U/N_s$ ;  $J_D = 1.0$ ,  $J_B = 0$ ; (b)  $g_{\text{eff}} = 1.0U/N_s$ , the boundaries are for  $g_{\text{eff}} = 1.0U/N_s$ , 0, and  $-1.0U/N_s$ ;  $J_D = 0$ ,  $J_B = 0.05$ ; (a,b)  $N_s = 100$  and  $z = 6$  (3D); (c)  $g_{\text{eff}} = 0$ ,  $t_0/U = 0$ ; (d,e)  $g_{\text{eff}} = U/N_s$ ,  $J_D = 1.0$ ,  $J_B = 0$ ,  $t_0/U = 0$ .

cause the light fluctuations induce additional atom fluctuations, and, e.g., for minimized scattering both need to be suppressed, which leads to the extension of the MI regions (Fig. 2a). Moreover, in a quantum OL, atoms can potentially enter MI even without atomic interaction, or weakly repulsive SF can be stabilized by quantum correlations.

Regions between MI states are SFs with incommensurate filling. We find that in a quantum dynamical

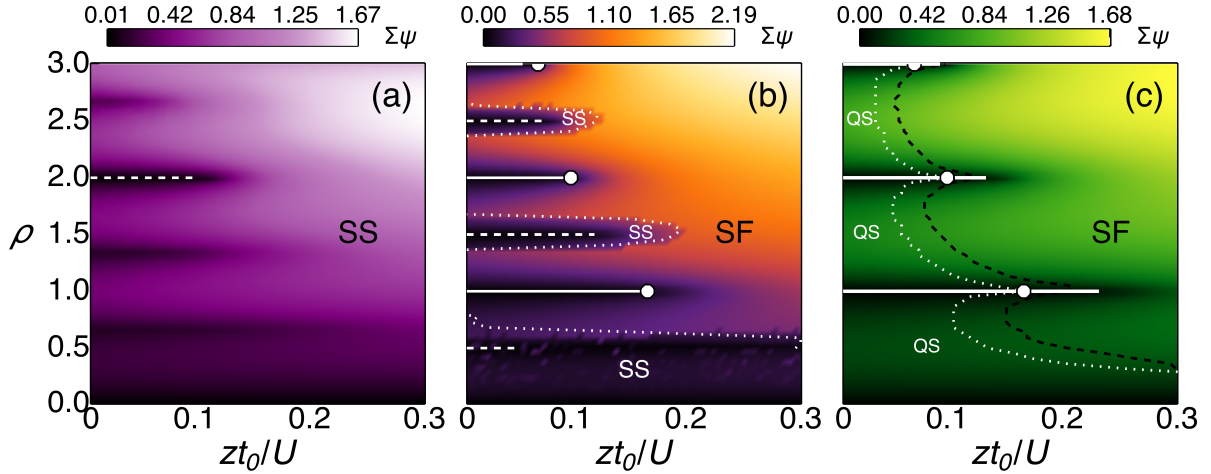


FIG. 3: **Emergence of density wave and supersolid phases in the diffraction minima of light with density scattering.** (a) Maximized scattering. Only giant DW and SS exist above the quantum critical point for light-matter coupling (no SF and MI phases). Phase diagram for the total order parameter of two density modes  $\Sigma\psi = |\psi_+|^2 + |\psi_-|^2$ , where  $\psi_{\pm}$  are the SF parameters of two modes. Here DW order parameter  $\Delta\rho = |\rho_+ - \rho_-|/2$  is always different from zero ( $\rho_{\pm}$  are the mean atom numbers per site in each mode). Dashed white lines correspond to DW insulators ( $\Sigma\psi = 0$ ,  $\Delta\rho \neq 0$ ), SS state occurs, when  $\Sigma\psi \neq 0$  and  $\Delta\rho \neq 0$ . (b) Maximized scattering. Total order parameter below the critical point for giant DW. Dashed lines at half-integer fillings correspond to DW insulators, white solid lines at integer fillings to MI; dotted lines are the boundaries between SS and SF. (c) Minimized scattering. Total order parameter, white lines correspond to MI. Quantum light fluctuations lead to the emergence of gapped SF (i.e. QS state). The boundaries of MI, SF, and MI can be tuned by the pump-cavity detuning. White points in (b) and (c) correspond to the MI-SF transition point without cavity light. Parameters: (a)  $g_{\text{eff}} = -1.25U/N_s$ , (b)  $g_{\text{eff}} = -0.5U/N_s$ , (c)  $g_{\text{eff}} = 10U/N_s$ , the boundaries are for  $g_{\text{eff}} = 10U/N_s$  and 0;  $J_D = 1.0$ ,  $J_B = 0$ ,  $N_s = 100$ ,  $z = 6$  (3D).

OL, this state is still gapless for the lowest particle-hole excitation, but importantly, becomes gapped with respect to all other excitations, and is thus topological. We call it the quantum superposition (QS) state, as it is a superposition of only  $n$  and  $n + 1$  fillings at each site. QS state may be important for quantum information purposes as a many-body gap-protected generalization of a two-level qubit system. In contrast to a regular SF, the gap opens because the effective chemical potential depends on the density and renormalizes to  $\mu - g_{\text{eff}}J_D^2((2N_s - 1)\rho - 1)$ . Without tunneling for  $g_{\text{eff}} > 0$ , the energy required to add a particle on top of the ground state is  $\Delta E_{\text{QS}}(\rho) = U\rho + g_{\text{eff}}J_D^2(2N_s\rho + 1)$  for incommensurate fillings between MI regions with fillings  $n$  and  $n + 1$ , with  $\rho = \frac{U}{2g_{\text{eff}}J_D^2N_s}(\frac{\mu}{U} - n)$  and on-site number fluctuations  $\Delta(\hat{n}_i) = (\rho - n)(1 - \rho + n)$ . For MI regions at commensurate density  $\rho = n$ , the gap is  $\Delta E_{\text{MI}}(n) = Un + g_{\text{eff}}J_D^2(2N_s n + 1)$  and  $\Delta(\hat{n}_i) = 0$ . This means that only occupations of the lowest particle-hole excitations are allowed between MI lobes. Similarly to SF-MI transition point, the boundaries of QS can be tuned (stabilized) due to the quantum correlations as  $U$  is renormalized (Fig. 2a). The key signature of these states is the emergence of SF shells even in a very deep OL due to harmonic confinement (Figs. 2c-e), while a system in prescribed lattices would be deep in MI regime showing

a standard "wedding cake" structure.

Choosing geometry [35], one can suppress the density scattering ( $J_D = 0$ ) and have all  $J_B$ 's equal. As no symmetry is broken, the bond self-organization does not emerge, but another semiclassical effect arises: tunneling is enhanced (suppressed) for maximum (minimum) scattering. This modifies the phase diagram (Fig. 2b), because of nonlinear coupling of the SF order parameter  $\psi = \langle \hat{b}_i \rangle$  to the tunneling amplitude  $t_0$ , which renormalizes to  $t_0 - 2zg_{\text{eff}}J_B^2N_s|\psi|^2$  ( $z$  is the coordination number).

Scattering light at  $90^\circ$ , one explicitly breaks the translational symmetry, which gets imprinted on the interaction of modes. Therefore, the system can support density waves (DWs) and novel bond orders. The simultaneous occurrence of SF and DW orders is a supersolid (SS) phase [28]. SS has been predicted due to the classical maximized light scattering [16, 17]. In the absence of bond scattering ( $J_{i,j} = (-1)^j J_D J_B = 0$ ), we have found that there exists a critical light-matter coupling ( $2|g_{\text{eff}}|N_s > U/2$ ), where MI and SF are entirely suppressed, which is a quantum critical point. The system only supports SS and DW due to incommensurability (Fig. 3a). It forms giant density waves with maximal amplitude constrained by the mean atom number per site and is described by a Devil's staircase [42]. Below this critical coupling, we have found that besides DW in-

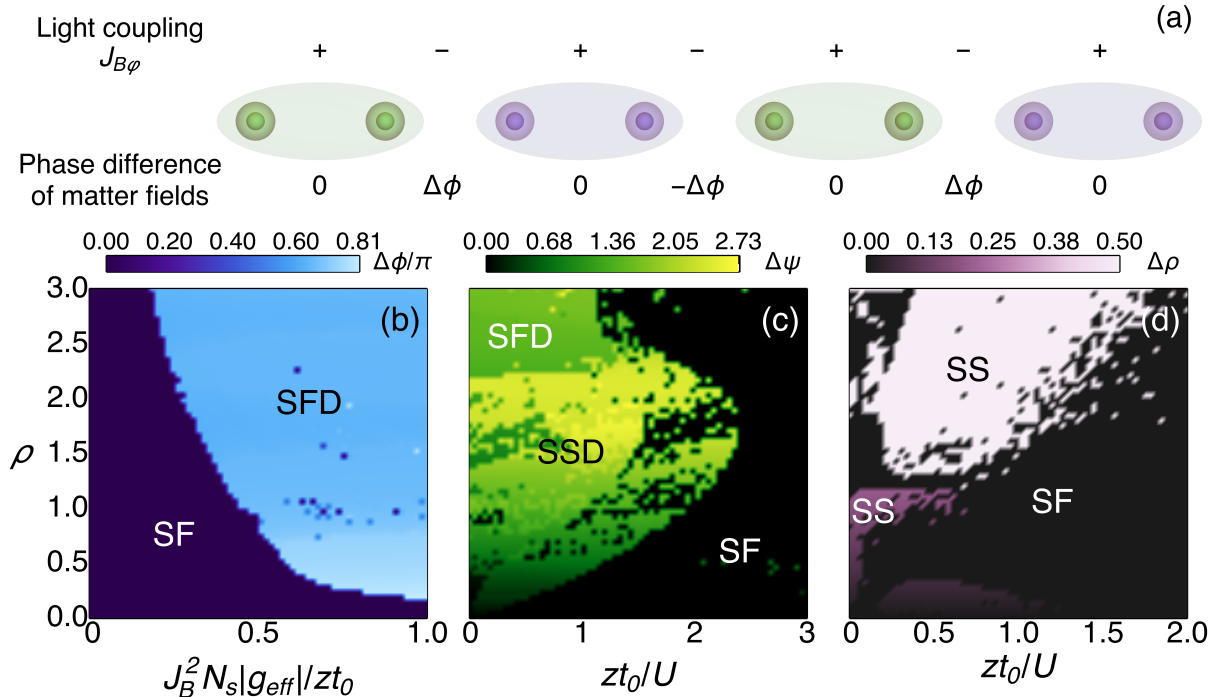


FIG. 4: **Emergent dimer phases and quantum-light-induced supersolids due to scattering from bonds.** (a) Dimer structure for maximized scattering. The matter-field phases alternate to compensate for imposed light-phase differences. (b) Phase diagram for the phase difference  $\Delta\phi$  between dimers without on-site interaction, when light scattering is maximized. (c) Phase diagram for the difference in order parameters  $\psi_{A/B}$  of the dimers  $\Delta\psi = ||\psi_A|^2 - |\psi_B|^2||/2$ . The formation of supersolid phases with dimer character occurs in addition to superfluid dimers, due to suppression of fluctuations by on-site interactions (maximized scattering). (d) Density wave order parameter  $\Delta\rho = |\rho_A - \rho_B||/2$  for minimized scattering. The density components  $\rho_{A/B}$  correspond to the atomic populations of the two effective light-induced modes. Density modulation originates essentially from the quantum light-matter correlations, regions with  $\Delta\rho \neq 0$  correspond to supersolid phases, while for  $\Delta\rho = 0$ , there is a normal superfluid (dark regions). Parameters: (b)  $U = 0$ , (c)  $g_{\text{eff}} = -25U/N_s$ , (d)  $g_{\text{eff}} = 25U/N_s$ ;  $J_D = 0$ ,  $J_B = 0.1$ ,  $N_s = 100$ , and  $z = 6$  (3D).

sulators present at half-integer fillings, MIs exist at commensurate filling (Fig. 3b).

For minimized light scattering ( $g_{\text{eff}} > 0$ ), the classical light cannot build up at all, and quantum fluctuations take the leading role. Similarly to the homogeneous case explained above, the gapped superfluid (QS) arises and the transition between MI, SF, and QS phases can be tuned (Fig. 3c). This provides absolute control of the DW order formation via the pump-cavity detuning. In analogous fermionic systems these are relevant for the stability of superconducting phases [43].

We find a novel phase transition, when light scattering from the bonds at  $90^\circ$  ( $J_{j,j+1} = (-1)^j J_B$ ,  $J_D = 0$ ) is maximized ( $g_{\text{eff}} < 0$ ). Even in the absence of on-site interaction, a transition from normal SF to the superfluid dimer (SFD) state appears. SFD is a SF state in which the complex order parameter has alternating (zero and non-zero) phase difference between pairs of sites, and its amplitude is modulated as well. This occurs because of the competition between the kinetic energy terms in the BH Hamiltonian, which promote a homogeneous SF

with zero phase difference between bonds, with the light-induced interaction that favours SF components with alternating phases across every other site (Fig. 4a). In other words, the quantum matter-fields self-organize in such a way, that the matter-field phase difference compensates for the imposed light-field phase difference (indeed, coefficients  $J_{j,j+1} = (-1)^j J_B$  reflect light scattering with phase difference  $\pi$  between nearest neighbour bonds), see Fig. 4a. The phase diagram is shown in Fig. 4b. Moreover, in the presence of on-site interaction the system supports a transition to the supersolid dimer (SSD) state, while insulating phases are suppressed (Fig. 4c). The density modulation occurs because of the interplay between SF imbalance and on-site number fluctuations. On-site interactions suppress fluctuations, thus locking the system in an imbalanced configuration. As tunneling increases, the SSD to normal SF transition occurs. For large  $U$ , as the density increases, the imbalance gets suppressed and there exists a SSD to SFD transition. Note, that multimode bond structure can have very non-trivial spatial overlap and dimers (and their multimode

generalizations) extended over many sites can be created. The dimer states can be used as fundamental units to engineer Hamiltonians of quantum spin-liquid states [34] via the Schwinger mapping [31].

Beyond that, we prove that there is a SS to SF transition that is solely driven by quantum correlations for minimized light scattering ( $g_{\text{eff}} > 0$ ), Fig. 4d. This occurs because the terms due to light-matter correlations in  $\hat{B}^\dagger \hat{B}$  are not shadowed by semiclassical effects, as there is no classical light build up. Two-point tunneling correlations introduce new terms in the BH model (see Methods), which couple densities at neighbouring sites only:  $\sum_{\langle i,j \rangle} \hat{n}_i \hat{n}_j$ , producing a DW instability even without strong light.

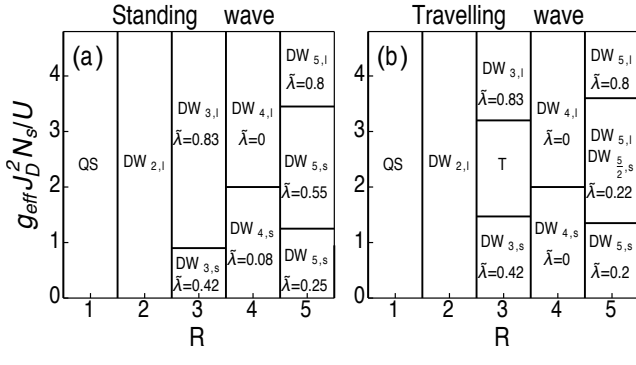


**FIG. 5: Phase diagram for multiple number of modes  $R$ .** Half-filling in the absence of tunneling. (a) Standing-wave cavity. (b) Travelling-wave cavity. The phases are characterized by the period of density-density correlations  $q$  (in units of lattice period) as  $\text{DW}_{q,l}$  and  $\text{DW}_{q,s}$ , where  $l$  denotes large and  $s$  small amplitude. In the supersolid state the largest eigenvalue scaled by the atom number,  $\tilde{\lambda} = \lambda/N > 0$ , shows the superfluid component. Density wave insulators have  $\tilde{\lambda} = 0$ . Surprisingly, at half-filling for  $R > 2$  supersolid state exists for large on-site interactions. A travelling-wave case has a transition region denoted by  $T$ , where the system is unable to lock to a definite configuration for DW order.  $\tilde{\lambda}$  is estimated from exact diagonalization results for small lattice sizes and is an upper bound to the value in the thermodynamic limit.

Going beyond two modes [36, 37], we calculate the phase diagram for increasing mode number  $R$ , using exact diagonalisation at half-filling with fixed particle number for strong  $U$  and maximized scattering (Fig. 5). We neglect tunneling ( $t_0/U = 0$ ,  $J_B = 0$ ), and the light-imposed coefficients are  $J_{j,j} = J_D \gamma(j)$ , where  $\gamma(j) = \cos(2\pi j/R)$  for a standing-wave cavity, and  $\gamma(j) = \exp(i2\pi j/R)$  for a travelling-wave cavity. We find that the system can support SS for  $R > 2$ , which are, remarkably, topologically protected, because the SF component is gapped, as was explained for the QS state. Moreover as the number of modes increases, the system has additional DWs and even their superpositions with SF order. In SS, there exist the off-diagonal long-range order (ODLRO). It is well known that SF component can be estimated by the largest eigenvalue  $\lambda$  of the one-body

reduced density matrix  $\rho^{(1)}$  [44, 45]. In the phase diagram, SSs have  $\lambda/N > 0$  with non-zero density-density correlations and DWs with  $\lambda/N = 0$ .

We now present the full entangled light-matter states (see Methods for the reconstruction procedure). For the multimode DWs ( $R \geq 2$ ) originating from density scattering,

$$|\Psi\rangle = \sum_{q=1}^{f(R)} \Gamma_{\varphi_q}^b(t) |\varphi_q\rangle_b |\alpha_{\varphi_q}\rangle_a, \quad (7)$$

where the subscript “ $a$ ” (“ $b$ ”) corresponds to the light (matter) part;  $\Gamma^b(t) = \exp(-i\mathcal{H}_{\text{eff}}^b t)$ , and  $\Gamma_{\varphi_q}^b |\varphi_q\rangle_b = \hat{\Gamma}^b |\varphi_q\rangle_b$ . The ground state of the effective Hamiltonian is  $|\Psi\rangle_b = \sum_{q=1}^{f(R)} |\varphi_q\rangle_b$ , where the number of DW components  $f(R) \geq 2$  depends on the sub-lattice structure generated (see Fig. 5). The coherent state amplitudes are  $\alpha_{\varphi_q} = CN_{\varphi_q}$  and depend on the projections  $N_{\varphi_q} |\varphi_q\rangle_b = \hat{D} |\varphi_q\rangle_b$ , where  $C = g_2/(\Delta_p + i\kappa)$ .

In case of dimers,

$$|\Psi\rangle = \sum_{q=1}^4 \Gamma_{\varphi_q}^b(t) |\varphi_q\rangle_b |CB_{\varphi_q}\rangle_a, \quad (8)$$

$$B_{\varphi_q} = N_s J_B \left( \frac{\phi_q + \phi_{q+2}}{2} - \frac{\phi_{q+1} + \phi_{q+3}}{2} \cos(\Delta\phi) \right), \quad (9)$$

$$\phi_q = |\psi_{q+1}^* \psi_q|, \quad (10)$$

$$\Delta\phi = \arg(\psi_{q+2}) - \arg(\psi_q) = \arg(\psi_{q+2}) - \arg(\psi_{q+1}), \quad (11)$$

where components  $q$  and  $q+4$  are the same and  $\psi_q = \langle \hat{b}_q \rangle$  is the order parameter corresponding to the mode  $\varphi_q$ . For SS dimers  $\phi_q \neq \phi_{q+2}$  and  $\phi_{q+1} \neq \phi_{q+3}$ , while for SF dimers  $\phi_q = \phi_{q+2}$  and  $\phi_{q+1} = \phi_{q+3}$ .

We see that both density and bond multimode self-organized states are represented by the superpositions of several macroscopic components. Using the quantum measurement of light, one can project the full states to one or several degenerate components, inducing novel states and dynamics [36]. In general, nonlinear light-matter coupling can generate non-classical states of light.

In conclusion, we have shown that quantum optical lattices offer a new tool to engineer nonlocal many-body interactions with light-induced structures. These interactions can break symmetries by design and imprint a pattern that governs the origin of many-body phases. The light and matter are entangled, forming non-trivial light-matter correlated states. We suggested how to generate not only multimode density patterns, but nonlocal patterns of matter-filled coherences as well (in particular, delocalized superfluid and supersolid dimers). Some of the states appear solely due to quantum fluctuations of light and matter, while no classical light can build up. Quantum optical lattices will certainly expand abilities of quantum simulators, which so far are based on classical

optical setups, and may influence quantum information processing. A pathway to realize our proposal is to combine several recent experimental breakthroughs: a BEC was trapped in a cavity, but without a lattice [2–4], and detection of light scattered from ultracold atoms in OL was performed, but without a cavity [46, 47]. Based on off-resonant scattering and thus being non-sensitive to a detailed atomic level structure, our approach can be extended to other arrays of natural or artificial quantum objects: spins, fermions, molecules (including biological ones), ions, atoms in multiple cavities, semiconductor or superconducting qubits.

### Acknowledgments

The work was supported by the EPSRC (EP/I004394/1).

### Methods

**Classical optical lattice model.** The Bose-Hubbard Hamiltonian is

$$\mathcal{H}^b = -t_0 \sum_{\langle i,j \rangle} (\hat{b}_i^\dagger \hat{b}_j + h.c.) - \mu \sum_i \hat{n}_i + \frac{U}{2} \sum_i \hat{n}_i (\hat{n}_i - 1), \quad (12)$$

where  $\langle i,j \rangle$  refers to nearest neighbour pairs,  $\hat{b}_i^\dagger$  ( $\hat{b}_i$ ) correspond to creation (annihilation) operators of bosonic atoms at the site  $i$  and the atom number operators are  $\hat{n}_i = \hat{b}_i^\dagger \hat{b}_i$ . The tunneling amplitude of the bosons is  $t_0$ , the on-site interaction is  $U$  and the chemical potential is  $\mu$ . The effective parameters of the Bose-Hubbard Hamiltonian with the cavity field can be calculated from the Wannier functions and are given by

$$t_0 = \int w(x - x_i) (\nabla^2 - V_{OL}(x)) w(x - x_j) d^n x, \quad (13)$$

$$J^{i,j} = \int w(x - x_i) u_c^*(x) u_p(x) w(x - x_j) d^n x, \quad (14)$$

where  $u_{c,p}(x)$  are the cavity and pump mode functions and  $w(x)$  are the Wannier functions. The classical optical lattice potential is given by  $V_{OL}(x)$ . Typical values for the amplitudes of couplings for the standing-wave potential  $V_{OL}(x) = V_0 \sin^2(2\pi x/\lambda)$  with  $V_0 \approx 5E_R$  are:  $t_0 \approx 1.9E_R$ ,  $|J_B^{i,j}| \approx 0.07$ ,  $|J_D^j| \approx 0.85$ , where  $E_R$  is the recoil energy. This has been calculated using real Wannier functions finding the maximally localised generalised Wannier states of the classical optical lattice using the MLGWS code [48].

**Light-induced interaction decomposition.** The light matter-correlations and dynamical terms in  $\hat{F}^\dagger \hat{F}$

can be decomposed in on-site mean-field as follows. The  $\hat{D}^\dagger \hat{D}$  term can be expanded as

$$\hat{D}^\dagger \hat{D} + h.c. \approx \sum_{\varphi, \varphi'} (J_{D,\varphi}^* J_{D,\varphi'} + c.c.) \langle \hat{N}_{\varphi'} \rangle (2\hat{N}_\varphi - \langle \hat{N}_\varphi \rangle), \\ + \delta \hat{D}^\dagger \hat{D} \quad (15)$$

$$\delta \hat{D}^\dagger \hat{D} = 2 \sum_{\varphi} |J_{D,\varphi}|^2 \delta \hat{N}_\varphi^2, \quad (16)$$

$$\delta \hat{N}_\varphi^2 = \sum_{i \in \varphi} (\hat{n}_i - \rho_i)^2, \quad (17)$$

where  $\langle \hat{N}_\varphi \rangle = \sum_{i \in \varphi} \rho_i$  is the mean number of atoms in the mode  $\varphi$  and  $\rho_i = \langle \hat{n}_i \rangle$  is the mean atom number at site  $i$ . The first term in Eq. (15) is due to the dynamical properties of the light field, these terms exhibit nonlocal coupling between light-induced modes. The terms in (16) signifies the light-matter correlations and contain the effect due to quantum fluctuations.

The  $\hat{B}^\dagger \hat{B}$  terms can be expanded as:

$$\hat{B}^\dagger \hat{B} + h.c. \approx \sum_{\varphi, \varphi'} (J_{B,\varphi}^* J_{B,\varphi'} + c.c.) \langle \hat{S}_{\varphi'} \rangle (2\hat{S}_\varphi - \langle \hat{S}_\varphi \rangle) \\ + \delta \hat{B}^\dagger \hat{B}, \quad (18)$$

$$\delta \hat{B}^\dagger \hat{B} = 2 \sum_{\varphi} |J_{B,\varphi}|^2 \delta \hat{S}_\varphi^2, \quad (19)$$

$$\delta \hat{S}_\varphi^2 = \sum_{\langle i,j \rangle \in \varphi} ((\hat{b}_i^\dagger \hat{b}_j + h.c. - \langle \hat{b}_i^\dagger \hat{b}_j + h.c. \rangle)^2 \\ + \sum_{\langle i,j,k \rangle \in \varphi} (\hat{b}_i^\dagger \hat{b}_k^\dagger (\hat{b}_j)^2 + (\hat{b}_j^\dagger)^2 \hat{b}_i \hat{b}_k + 2\hat{n}_i \hat{b}_k^\dagger \hat{b}_j + \hat{b}_k^\dagger \hat{b}_j \\ - (\hat{b}_k^\dagger \hat{b}_j + \hat{b}_i^\dagger \hat{b}_k + h.c.) \langle \hat{b}_i^\dagger \hat{b}_j + h.c. \rangle), \quad (20)$$

where  $\langle i,j,k \rangle$  refers to  $i,j$  nearest neighbours and  $k$  is a nearest neighbour to the pair  $\langle i,j \rangle$ . The first term in (18) is due to the dynamical properties of the light field and (20) are due to light-matter correlations. The on-mode light matter correlations  $\hat{B}_\varphi^\dagger \hat{D}_\varphi + \hat{D}_\varphi^\dagger \hat{B}_\varphi$  reduce to on-site covariances per mode. In the above we have decorrelated products of operators at different sites such that  $\hat{\xi}_i \hat{\nu}_j \approx \langle \hat{\xi}_i \rangle \hat{\nu}_j + \langle \hat{\nu}_j \rangle \hat{\xi}_i - \langle \hat{\xi}_i \rangle \langle \hat{\nu}_j \rangle$ , where  $\hat{\xi}$  or  $\hat{\nu}$  are combinations of  $\hat{b}^\dagger$  or  $\hat{b}$  operators at a given site. The expectation value of the bond operators reduces to  $\langle \hat{S}_\varphi \rangle = \sum_{\langle i,j \rangle \in \varphi} (\psi_i^\dagger \psi_j + \psi_j^\dagger \psi_i)$ , which is the sum of products of order parameters at nearest neighbour sites in the light-induced mode  $\varphi$ .

**Effective Hamiltonians.** The effective Hamiltonian

considering only diagonal coupling ( $\hat{D}^\dagger \hat{D} + h.c.$ ) is

$$\mathcal{H}_{\text{eff}}^b = -t_0 \sum_{\langle i,j \rangle} (\hat{b}_i^\dagger \hat{b}_j + h.c.) \quad (21)$$

$$+ \sum_{\varphi} \left[ \sum_{i \in \varphi} \left( \frac{U_{\varphi}}{2} \hat{n}_i (\hat{n}_i - 1) - 2g_{\text{eff}} |J_{D,\varphi}|^2 \rho_i \hat{n}_i \right) \right. \\ \left. - \mu_{\varphi} \hat{N}_{\varphi} - g_{\text{eff}} c_{D,\varphi} \right],$$

$$\mu_{\varphi} = \mu - g_{\text{eff}} \gamma_{D,\varphi}, \quad (22)$$

$$U_{\varphi} = U + 2g_{\text{eff}} |J_{D,\varphi}|^2, \quad (23)$$

with  $\gamma_{D,\varphi} = \sum_{\varphi'} (J_{D,\varphi}^* J_{D,\varphi'} + c.c.) \langle \hat{N}_{\varphi'} \rangle - |J_{D,\varphi}|^2$  and  $c_{D,\varphi} = \sum_{\varphi'} (J_{D,\varphi}^* J_{D,\varphi'} + c.c.) \langle \hat{N}_{\varphi'} \rangle \langle \hat{N}_{\varphi} \rangle / 2 - |J_{D,\varphi}|^2 \sum_{i \in \varphi} \rho_i^2$ . The many-body interaction  $U_{\varphi}$  and the chemical potential  $\mu_{\varphi}$  inherit the pattern induced by the quantum potential that depends on light-induced mode structure given by  $\varphi$ .

In the case of only off-diagonal bond scattering, we have

$$\mathcal{H}_{\text{eff}}^b = \sum_{\varphi} \left[ -t_{\varphi} \hat{S}_{\varphi} + g_{\text{eff}} |J_{B,\varphi}|^2 \delta \hat{S}_{\varphi}^2 - g_{\text{eff}} c_{B,\varphi} \right] \quad (24)$$

$$+ \sum_i \left( \frac{U}{2} \hat{n}_i (\hat{n}_i - 1) - \mu \hat{n}_i \right), \quad (25)$$

$$t_{\varphi} = t_0 - g_{\text{eff}} \gamma_{B,\varphi}, \quad (26)$$

with  $\gamma_{B,\varphi} = \sum_{\varphi'} (J_{B,\varphi}^* J_{B,\varphi'} + c.c.) \langle \hat{S}_{\varphi'} \rangle$  and  $c_{B,\varphi} = \sum_{\varphi'} (J_{B,\varphi}^* J_{B,\varphi'} + c.c.) \langle \hat{S}_{\varphi'} \rangle \langle \hat{S}_{\varphi} \rangle / 2$ . The effective tunneling amplitude  $t_{\varphi}$  couples the SF components of all the light-induced modes  $\varphi$ . The terms due to  $\delta \hat{S}_{\varphi}^2$  induce nontrivial coupling between nearest neighbour sites and lead to the formation of a density wave instability with more than one light-induced mode.

The effective coupling parameters  $\gamma_{D/B,\varphi}$  depend implicitly on all the light induced modes giving nonlocal coupling via the expectation values of the operators  $\hat{S}_{\varphi}$  and  $\hat{N}_{\varphi}$ .

In the specific case of a single light-induced mode component in the diffraction maxima, we have:  $\gamma_D = 2J_D^2(N_s \rho - 1/2)$  and  $\gamma_B = 2zJ_B^2N_s|\psi|^2$  with  $\rho = \langle \hat{n}_i \rangle$  and  $\psi = \langle \hat{b}_i \rangle$  for all sites and  $z$  is the coordination number. This gives the effective tunneling amplitude  $t_{\varphi} = t_0 - 2zg_{\text{eff}}J_B^2N_s|\psi|^2$ , the effective chemical potential  $\mu_{\varphi} = \mu - g_{\text{eff}}J_D^2(2(N_s - 1)\rho - 1)$  [where we have added all onsite density terms], and the effective interaction strength  $U_{\varphi} = U + 2g_{\text{eff}}J_D^2$ .

The case for two components in the diffraction minima in diagonal density scattering reduces to  $\gamma_{D,\pm} = \pm J_D^2 N_s \Delta \rho - J_D^2$  with  $\Delta \rho = (\rho_+ - \rho_-)/2$ , where  $\rho_{\pm}$  correspond to the mean atom numbers of each of the two light-induced modes. Thus, the effective chemical potential is  $\mu_{\pm} = \mu \pm g_{\text{eff}}J_D^2 N_s \Delta \rho - g_{\text{eff}}J_D^2$  and  $U_{\pm} = U + 2g_{\text{eff}}J_D^2$ . For off-diagonal coupling the situation is more subtle and this requires four components,

$$t_{\varphi_q} = t_0 - g_{\text{eff}} \gamma_{B,\varphi_q}, \quad (27)$$

$$\gamma_{B,\varphi_q} = \frac{z(-1)^{q+1} J_B^2 N_s}{2} \sum_{q'=1}^4 (-1)^{q'+1} (\psi_{q'}^* \psi_{q'+1} + c.c.), \quad (28)$$

where the component  $q+4$  is the same as  $q$ . This is the origin of dimer states discussed in the main text.

**The full entangled light-matter state.** The full light-matter state can be found using an alternative procedure to [6, 38] using rotations over the Hilbert space via canonical transformations [45]. We obtain

$$|\Psi\rangle \approx \sum_{\varphi_q} \Gamma_{\varphi_q}^b(t) |\varphi_q\rangle_b |\alpha_{\varphi_q}\rangle_a, \quad (29)$$

where the subscript “ $a$ ” (“ $b$ ”) corresponds to the light (matter) part. The coherent state amplitudes are  $\alpha_{\varphi_q} = CF_{\varphi_q}$ , where  $C = g_2/(\Delta_p + i\kappa)$ . These amplitudes depend on the projection  $F_{\varphi_q} |\varphi_q\rangle_b = \hat{F} |\varphi_q\rangle_b$ , that corresponds to the steady state component  $|\varphi_q\rangle_b$  of the effective matter Hamiltonian  $\mathcal{H}_{\text{eff}}^b$ . The phase factor is due to the time evolution of the effective matter Hamiltonian:  $\hat{\Gamma}^b(t) = \exp(-i\mathcal{H}_{\text{eff}}^b t)$ ,  $\Gamma_{\varphi_q}^b |\varphi_q\rangle_b = \hat{\Gamma}^b |\varphi_q\rangle_b$ . This is accurate in the limits  $|\kappa/\Delta_p| \ll 1$ ,  $|t_0/\Delta_p| \ll 1$ ,  $|J_B E_R/\Delta_p| \ll 1$ .

**Numerical methods.** Numerical simulations of the effective Hamiltonian have been carried out by doing spatial mode decoupling theory truncated in Hilbert space using the Gutzwiller ansatz with self-consistent conditions with light-induced interaction given by Eqs. (15) and (18). The problem is solved as a multimode constrained nonlinear optimisation problem in  $2R(f+1)$  dimensions and  $3R$  constraints with  $R$  being the number of light-induced modes and  $f$  is the filling factor of the mode occupation. For our parameter range it is sufficient to consider  $f = \rho + 2$ . Exact diagonalization calculations are done on the Hamiltonian (4).

---

[1] Lewenstein, M., Sanpera, A. & Ahufinger, V. *Ultracold atoms in optical lattices: Simulating Quantum Many-Body Systems*. Oxford University Press (2012).  
[2] Baumann, K., Guerlin, C., Brennecke, F. & Esslinger, T.

Dicke quantum phase transition with a superfluid gas in an optical cavity. *Nature* **464**, 1301-1306 (2010).  
[3] Wolke, M., Klinner, J., Kessler, H. & Hemmerich, A. Cavity cooling below the recoil limit. *Science* **337**, 85-87

(2012).

[4] Schmidt, D., Tomczyk, H., Slama, S. & Zimmermann, C. Dynamical Instability of a Bose-Einstein Condensate in an Optical Ring Resonator. *Phys. Rev. Lett.* **112**, 115302 (2014).

[5] Ritsch, H., Domokos, P., Brennecke, F. & Esslinger, T. Cold atoms in cavity-generated dynamical optical potentials. *Rev. Mod. Phys.* **85**, 553-601 (2013).

[6] Maschler, C., Mekhov, I. B. & Ritsch, H. Ultracold atoms in optical lattices generated by quantized light fields. *Eur. Phys. J. D* **46**, 545-560 (2008).

[7] Vukics A., Maschler, C. & Ritsch, H. Microscopic physics of quantum self-organization of optical lattices in cavities. *New J. Phys.* **9**, 255 (2007).

[8] Krämer, S. & Ritsch, H. Self-ordering dynamics of ultracold atoms in multicolored cavity fields. *Phys. Rev. A* **90**, 033833 (2014).

[9] Winterauer, D. J., Niedenzu, W. & Ritsch, H. Multi-stable particle-field dynamics in cavity-generated optical lattices. arXiv:1503.07044.

[10] Kónya, G., Szirmai, G. & Domokos, P. Damping of quasi-particles in a Bose-Einstein condensate coupled to an optical cavity. *Phys. Rev. A* **90**, 013623 (2014).

[11] Landig, R., Brennecke, F., Mottl, R., Donner, T. & Esslinger, T. Measuring the dynamic structure factor of a quantum gas undergoing a structural phase transition. arXiv:1503.05565.

[12] Domokos, P. & Ritsch, H. Collective Cooling and Self-Organization of Atoms in a Cavity. *Phys. Rev. Lett.* **89**, 253003 (2002).

[13] Black, A. T., Chan, H. W. & Vuletić, V. Observation of Collective Friction Forces due to Spatial Self-Organization of Atoms: From Rayleigh to Bragg Scattering. *Phys. Rev. Lett.* **91**, 203001 (2003).

[14] Larson, J., Damski, B., Morigi, G. & Lewenstein, M. Mott-insulator states of ultracold atoms in optical resonators. *Phys. Rev. Lett.* **100**, 050401 (2008).

[15] Fernandez-Vidal, S., De Chiara, G., Larson, J. & Morigi, G. Quantum ground state of self-organized atomic crystals in optical resonators. *Phys. Rev. A* **81**, 043407 (2010).

[16] Li, Y., He, L. & Hofstetter, W. Lattice-supersolid phase of strongly correlated bosons in an optical cavity. *Phys. Rev. A* **87**, 051604(R) (2013).

[17] Bakhtiari, M. R., Hemmerich, A., Ritsch, H. & Thorwart, M. Nonequilibrium Phase Transition of Interacting Bosons in an Intra-Cavity Optical Lattice. *Phys. Rev. Lett.* **114**, 123601 (2015).

[18] Habibian, H., Winter, A., Paganelli, S., Rieger, H. & Morigi, G. Bose-Glass Phases of Ultracold Atoms due to Cavity Backaction. *Phys. Rev. Lett.* **110**, 075304 (2013).

[19] Gopalakrishnan, S., Lev, B. S. & Goldbart, P. M. Emergent crystallinity and frustration with Bose-Einstein condensates in multimode cavities. *Nat. Phys.* **5**, 845-850 (2009).

[20] Müller, M., Strack, P. & Sachdev, S. Quantum charge glasses of itinerant fermions with cavity-mediated long-range interactions. *Phys. Rev. A* **86**, 023604 (2012).

[21] Mekhov, I. B., Maschler, C. & Ritsch, H. Probing quantum phases of ultracold atoms in optical lattices by transmission spectra in cavity quantum electrodynamics. *Nat. Phys.* **3**, 319-323 (2007).

[22] Mekhov, I. B. & Ritsch, H. Quantum optics with ultracold quantum gases: towards the full quantum regime of the light-matter interaction. *J. Phys. B: At. Mol. Opt. Phys.* **45**, 102001(2012).

[23] Bonnes, L., Charrier, D. & Läuchli, A. M. Dynamical and steady-state properties of a Bose-Hubbard chain with bond dissipation: A study based on matrix product operators. *Phys. Rev. A* **90**, 033612 (2014).

[24] Labeyrie, G., et al. Optomechanical self-structuring in a cold atomic gas. *Nature Photon* **8**, 321325 (2014).

[25] Aspelmeyer, M., Kippenberg, T. J. & Marquardt, F. Cavity optomechanics. *Rev. Mod. Phys.* **86**, 1391-1452 (2014).

[26] Zeng, B. & Wen, X.-G. Gapped quantum liquids and topological order, stochastic local transformations and emergence of unitarity. *Phys. Rev. B* **91**, 125121 (2015).

[27] Grüner, G. The dynamics of charge-density waves. *Rev. Mod. Phys.* **60**, 1129-1181 (1988).

[28] Cinti, F., Macrì, T., Lechner, W., Pupillo, G. & Pohl, T. Defect-induced supersolidity with soft-core bosons. *Nat. Commun.* **5**, 02 (2014).

[29] Zohar, E., Cirac, J. I., & Reznik, B. Cold-Atom Quantum Simulator for SU(2) Yang-Mills Lattice Gauge Theory. *Phys. Rev. Lett.* **110**, 125304 (2013).

[30] Stannigel, K., et al. Constrained Dynamics via the Zeno Effect in Quantum Simulation: Implementing Non-Abelian Lattice Gauge Theories with Cold Atoms. *Phys. Rev. Lett.* **112**, 120406 (2014).

[31] Auerbach, A. *Interacting Electrons and Quantum Magnetism*, Springer-Verlag, New York (1994)

[32] Bloch, I., Dalibard, J. & Sylvain, J. Quantum simulations with ultracold quantum gases. *Nat. Phys.* **8** 267-276 (2012).

[33] Witten, E. Global aspects of current algebra *Nuclear Physics B* **223**, 422 (1983)

[34] Balents, L. Spin liquids in frustrated magnets. *Nature* **464**, 199-208 (2010).

[35] Kozlowski, W., Caballero-Benitez, S. F. & Mekhov, I. B. Probing Matter-Field and Atom-Number Correlations in Optical Lattices by Global Nondestructive Addressing. arXiv:1411.7567.

[36] Mazzucchi, G., Kozlowski, W., Caballero-Benitez, S. F., Elliott, T. J. & Mekhov, I. B. Quantum Measurement-induced Dynamics of Many-Body Ultracold Bosonic and Fermionic Systems in Optical Lattices. arXiv:1503.08710.

[37] Elliott, T. J., Kozlowski, W., Caballero-Benitez, S. F. & Mekhov, I. B. Multipartite Entangled Spatial Modes of Ultracold Atoms Generated and Controlled by Quantum Measurement. *Phys. Rev. Lett.* **114**, 113604 (2015).

[38] Mekhov, I. B. & Ritsch, H. Quantum optics with quantum gases: Controlled state reduction by designed light scattering. *Phys. Rev. A* **80** 013604 (2009).

[39] Mekhov, I. B. & Ritsch, H. Quantum optics with quantum gases. *Laser Phys.* **19**, 610-615 (2009).

[40] Mekhov, I. B. & Ritsch, H. Quantum optical measurements in ultracold gases: Macroscopic Bose-Einstein condensates. *Laser Phys.* **20**, 694-699 (2010).

[41] Baumann, K., Mottl, R., Brennecke, F. & Esslinger, T. Exploring Symmetry Breaking at the Dicke Quantum Phase Transition. *Phys. Rev. Lett.* **107**, 140402 (2011).

[42] Bak, P. The Devil's Staircase. *Physics Today* **39** (12), 38 (1986).

[43] da Silva Neto, E. H., et al. Ubiquitous Interplay Between Charge Ordering and High-Temperature Superconductivity in Cuprates. *Science* **343**, 393-396 (2014).

[44] Yang, C. N. Concept of Off-Diagonal Long-Range Order

and the Quantum Phases of Liquid He and of Superconductors. *Rev. Mod. Phys.* **34**, 694-704 (1962).

[45] Mahan, G. D. *Many Particle Physics*. Plenum, New York, 3rd edition, (2000).

[46] Hirokazu, M., et al. Bragg Scattering as a Probe of Atomic Wave Functions and Quantum Phase Transitions in Optical Lattices. *Phys. Rev. Lett.* **107**, 175302 (2011).

[47] Weitenberg, C., et al. Coherent Light Scattering from a Two-Dimensional Mott Insulator. *Phys. Rev. Lett.* **106**, 215301 (2011).

[48] Walters, R., Cotugno, G., Johnson, T. H., Clark, S. R. & Jaksch, D. *Ab initio derivation of Hubbard models for cold atoms in optical lattices* . *Phys. Rev. A* **87**, 043613 (2013).